Survival of the Dirac Points in Rippled Graphene

Lucian Covaci and Mona Berciu

Department of Physics and Astronomy, University of British Columbia, Vancouver, British Columbia, Canada, V6T 1Z1

(Received 31 March 2008; published 26 June 2008)

We study the effects of the rippling of a graphene sheet on quasiparticle dispersion. This is achieved using a generalization to the honeycomb lattice of the momentum average approximation, which is accurate for all coupling strengths and at all energies. We show that even though the position of the Dirac points may move and the Fermi speed can be renormalized significantly, quasiparticles with very long lifetimes survive near the Dirac points even for very strong couplings.

DOI: 10.1103/PhysRevLett.100.256405 PACS numbers: 71.38.−k, 81.05.Uw

Graphene [1] has been a hot research topic recently [2], primarily due to its Dirac points and the new paradigm of relativisticlike electron dispersion in their vicinity. Such dispersion is predicted by almost any hopping model on the two-dimensional (2D) honeycomb lattice. However, 2D systems should not have long-range order [3], and indeed, free-standing graphene sheets are rippled [4]. In epitaxial graphene [5], coupling to substrate phonons becomes important. Both of these can be modeled as Holstein-like coupling of electrons to out-of-plane optical phonons [6]. Here we investigate the effect of such coupling on the electronic dispersion.

This issue is important because we know from studies of Holstein polarons on simple cubic lattices that even weak-to-moderate electron-phonon coupling has significant effects [7]; while a polaron band with infinite lifetime appears at very low energies, the higher-energy spectral weight broadens considerably. In other words, phonon emission and absorption leads to very short lifetimes for all higher-energy states. This raises the possibility that the Dirac points, which are at high energies above the bottom of the band, may also be ''washed out'' into an incoherent and featureless background.

We study this problem, for a single electron. Of course, graphene is a half-metal and phonon-mediated electron-electron interactions may lead to further broadening. We assume that such effective interactions, like the Coulomb interactions, have little effect on lifetimes [8].

Our results show that well-defined Dirac points with long-lived quasiparticles are preserved even for extremely strong electron-phonon coupling, where most of the rest of the spectrum is highly incoherent. Thus, these most interesting features are very robust, although their energies are shifted somewhat and the slope may be renormalized. These results justify why one can ignore the rippling effects and assume a 2D lattice with long-lived quasiparticles, as has been done so far. This provides a valid description near the Dirac points, but would fail if the Fermi energy was anywhere else.

We use a generalization of the momentum average (MA) approximation [9] to calculate the single-electron Green's function. MA was shown to be accurate for the entire spectrum (not just low energies) for all coupling strengths and in all dimensions, for such problems [10,11]. This is so because the MA spectral weight obeys exactly a significant number of sum rules, and is accurate for all higher order ones. It can also be systematically improved [11]. We use here the generalizations of the $\mathrm{MA}^{(0)}$ and $\mathrm{MA}^{(1)}$ levels. There is no difference between their predictions near the Dirac points, showing that convergence is reached and we need not go to a higher level. The results shown are from $\mathrm{MA}^{(1)}$, whose spectral weight fulfills exactly the first 8 sum rules.

Consider the honeycomb lattice, with basis vectors $\mathbf{a}_{1,2} = 3a/2(1, \pm 1/\sqrt{3})$, and the three nearest neighbors of any site defined by $\boldsymbol{\delta}_1 = (a, 0)$, $\boldsymbol{\delta}_{2,3} = -a/2(1, \sqrt{3})$. In $\mathbf{k}$ space, the Holstein Hamiltonian for an electron coupled to an out-of-plane optical phonon mode is

$$\mathcal{H} = \sum_{\mathbf{k}} (\phi_{\mathbf{k}} c_{\mathbf{k}}^{\dagger} d_{\mathbf{k}} + \mathrm{H.c.}) + \Omega \sum_{\mathbf{q}} (b_{\mathbf{q}}^{\dagger} b_{\mathbf{q}} + B_{\mathbf{q}}^{\dagger} B_{\mathbf{q}}) + \frac{g}{\sqrt{N}} \sum_{\mathbf{k},\mathbf{q}} [c_{\mathbf{k}-\mathbf{q}}^{\dagger} c_{\mathbf{k}} (b_{\mathbf{q}}^{\dagger} + b_{-\mathbf{q}}) + d_{\mathbf{k}-\mathbf{q}}^{\dagger} d_{\mathbf{k}} (B_{\mathbf{q}}^{\dagger} + B_{-\mathbf{q}})],$$

where $c^{\dagger}$ and $b^{\dagger}$ ($d^{\dagger}$ and $B^{\dagger}$) create electrons, respectively, phonons on the two sublattices. The first term is the kinetic energy of the electron for nearest-neighbor hopping, with $\phi_{\mathbf{k}} = -t \sum_{i=1}^{3} e^{i\mathbf{k}\boldsymbol{\delta}_i}$. Generalization to other models is straightforward. The second term describes the optical phonons of frequency Ω, for the two sublattices. The Holstein coupling of the electron to phonons on the same site is described by the last term, g being the coupling strength. All $\mathbf{k}$ sums are over the Brillouin zone (BZ), defined by the reciprocal lattice vectors $\mathbf{b}_{1,2} = 2\pi/3a(1, \pm\sqrt{3})$. We set $t = 1$, $\hbar = 1$. $N \to \infty$ is the number of unit cells.

Given the bipartite lattice, the single-electron Green's function can be defined as a (2×2) matrix:

$$\bar{G}(\mathbf{k}, \omega) = \langle 0 | \begin{pmatrix} c_{\mathbf{k}} \\ d_{\mathbf{k}} \end{pmatrix} \hat{G}(\omega) (c_{\mathbf{k}}^{\dagger} \; d_{\mathbf{k}}^{\dagger}) | 0 \rangle = \begin{pmatrix} \langle 0 | c_{\mathbf{k}} \hat{G}(\omega) c_{\mathbf{k}}^{\dagger} | 0 \rangle & \langle 0 | c_{\mathbf{k}} \hat{G}(\omega) d_{\mathbf{k}}^{\dagger} | 0 \rangle \\ \langle 0 | d_{\mathbf{k}} \hat{G}(\omega) c_{\mathbf{k}}^{\dagger} | 0 \rangle & \langle 0 | d_{\mathbf{k}} \hat{G}(\omega) d_{\mathbf{k}}^{\dagger} | 0 \rangle \end{pmatrix}, \quad (1)$$

where $\hat{G}(\omega) = (\omega + i\delta - \mathcal{H})^{-1}$ and $|0\rangle$ is the vacuum.

The resolvent for the free electron is $\hat{G}_0(\omega) = (\omega + i\delta - \mathcal{H}_0)^{-1}$, where $\mathcal{H}_0 = \mathcal{H}|_{g=0}$. The free-electron propagator can be calculated straightforwardly:

$$\bar{G}_0(\mathbf{k}, \omega) = \begin{pmatrix} G_{0S}(\mathbf{k}, \omega) & e^{i\xi(k)} G_{0A}(\mathbf{k}, \omega) \\ e^{-i\xi(k)} G_{0A}(\mathbf{k}, \omega) & G_{0S}(\mathbf{k}, \omega) \end{pmatrix},$$

where the symmetric and antisymmetric parts are

$$G_{0S,A}(\mathbf{k}, \omega) = \frac{1}{2}\left(\frac{1}{\omega + i\delta - |\phi(\mathbf{k})|} \pm \frac{1}{\omega + i\delta + |\phi(\mathbf{k})|} \right) \tag{2}$$

while the phase factor is $e^{i\xi(\mathbf{k})} = \phi_{\mathbf{k}}/|\phi_{\mathbf{k}}|$. As expected in a bipartite lattice, two symmetric bands arise with energy dispersions given by $E_{\mathbf{k}\pm} = \pm|\phi_{\mathbf{k}}|$ where $|\phi_{\mathbf{k}}| = [1 + 4\cos^2(\frac{\sqrt{3}}{2} k_y a) + 4\cos(\frac{\sqrt{3}}{2} k_y a)\cos(\frac{3}{2} k_x a)]^{1/2}$. In the first Brillouin zone, the dispersion vanishes at the two Dirac points K, K' located at $2\pi/3a(1, \pm 1/\sqrt{3})$.

We now describe briefly the MA$^{(1)}$ approximation for calculating $\bar{G}(\mathbf{k}, \omega)$, emphasizing the differences from the derivation of Ref. [11], due to the two-site basis. Like there, first we generate the equations of motion for this Green's function, and all the higher order ones it is linked to. This is achieved by using repeatedly Dyson's equation $\hat{G}(\omega) = \hat{G}_0(\omega) + \hat{G}(\omega)\hat{V}\hat{G}_0(\omega)$, where $\hat{V} = \mathcal{H} - \mathcal{H}_0$ is the electron-phonon interaction. The first equation is

$$\bar{G}(\mathbf{k}, \omega) = \left[1 + \frac{g}{\sqrt{N}} \sum_{\mathbf{q}_1} \bar{F}_1(\mathbf{k}, \mathbf{q}_1, \omega) \right] \bar{G}_0(\mathbf{k}, \omega), \tag{3}$$

where $\bar{F}_1(\mathbf{k}, \mathbf{q}_1, \omega)$ is the one-phonon Green's function:

$$\bar{F}_1(\mathbf{k}, \mathbf{q}_1, \omega) = \langle 0| \begin{pmatrix} c_{\mathbf{k}} \\ d_{\mathbf{k}} \end{pmatrix} \hat{G}(\omega) \begin{pmatrix} c^\dagger_{\mathbf{k}-\mathbf{q}_1} b^\dagger_{\mathbf{q}_1} & d^\dagger_{\mathbf{k}-\mathbf{q}_1} B^\dagger_{\mathbf{q}_1} \end{pmatrix} |0\rangle.$$

The equation of motion for $\bar{F}_1$ links it back to $\bar{G}$, but also to two-phonon Green's functions. The two phonons are both on the same sublattice as the electron, or one may be on the other sublattice. The equations for these link them back to $\bar{F}_1$, but also to a new one-phonon Green's function $\bar{F}^*_1$, which has the phonon on the different sublattice than the electron. And, of course, to a multitude of three-phonon Green's functions. And so on and so forth. All these higher-order Green's functions must be proportional to the 2×2 matrix $\bar{G}(\mathbf{k}, \omega)$ [11], so it is convenient to rescale them accordingly, e.g., $\bar{f}_1(\mathbf{k}, \mathbf{q}_1, \omega) = g\sqrt{N}\bar{G}^{-1}(\mathbf{k}, \omega) \times \bar{F}_1(\mathbf{k}, \mathbf{q}_1, \omega)$, and similarly for all the other ones (see below). Combining this with Eq. (3), we find the standard solution $\bar{G}(\mathbf{k}, \omega) = [\bar{G}_0^{-1}(\mathbf{k}, \omega) - \bar{\Sigma}(\mathbf{k}, \omega)]^{-1}$, where the self-energy is

$$\bar{\Sigma}(\mathbf{k}, \omega) = \frac{1}{N} \sum_{\mathbf{q}_1} \bar{f}_1(\mathbf{k}, \mathbf{q}_1, \omega). \tag{4}$$

Our task is thus to calculate the momentum average over the first Brillouin zone of the generalized Green's function $\bar{f}_1(\mathbf{k}, \mathbf{q}_1, \omega)$. As just discussed, this is the solution of an infinite system of coupled equations of motion. We cannot solve it exactly, so we proceed to make simplifications. At the MA$^{(0)}$ level, we replace all free propagators that appear in all these equations by their momentum averages over the first Brillouin zone. Within MA$^{(1)}$, we keep the equations for $\bar{f}_1$ and $\bar{f}^\star_1$ unchanged, and make the MA approximation only from the second level on, i.e., for free propagators of energy $\omega - n\Omega$ where $n \geq 2$. Either of these approximations allows us to solve the resulting equations of motion exactly. We proceed to discuss the MA$^{(1)}$ solution in more detail.

As for the simpler case presented at length in Ref. [11], the simplified MA$^{(1)}$ equations of motion can be solved in terms of total (and partial) momentum averages of these higher Green's functions, over all (all minus one) of their phonons' momenta. After such total (partial) averages, only contributions from Green's function which have all (all except one) of their phonons on the same sublattice as the electron are nonvanishing. This is because one can easily check, using Fourier transforms, that

$$\sum_{\mathbf{q}_1, \ldots, \mathbf{q}_n} c^\dagger_{\mathbf{k}-\mathbf{q}_1-\ldots-\mathbf{q}_n} b^\dagger_{\mathbf{q}_1} \ldots b^\dagger_{\mathbf{q}_n} = N^{(n-1/2)} \sum_i e^{i\mathbf{k}\cdot\mathbf{R}_i} c^\dagger_i (b^\dagger_i)^n.$$

If any phonon is on the other sublattice, the sum over its momentum vanishes, since it cannot be at the same site as the electron. This shows the variational meaning of these approximations [11,12]: in MA$^{(0)}$, a phonon cloud can appear at any one site. In MA$^{(1)}$ there can also be an additional phonon anywhere else in the system. MA$^{(1)}$ thus describes correctly the polaron + one-phonon continuum [11], but this is a very low-energy feature compared to the Dirac points. Diagrammatically, both sum all the self-energy diagrams, but each diagram is simplified [11].

To summarize, the only Green's functions whose total or partial averages remain finite are (after rescaling):

$$\bar{f}_n(\mathbf{q}_1, \ldots, \mathbf{q}_n) = g^n N^{(n/2)} \bar{G}^{-1}(\mathbf{k}, \omega) \langle 0| \begin{pmatrix} c_{\mathbf{k}} \\ d_{\mathbf{k}} \end{pmatrix} \hat{G} \begin{pmatrix} c^\dagger_{\mathbf{k}-\mathbf{q}_T} b^\dagger_{\mathbf{q}_1} \ldots b^\dagger_{\mathbf{q}_n} & d^\dagger_{\mathbf{k}-\mathbf{q}_T} B^\dagger_{\mathbf{q}_1} \ldots B^\dagger_{\mathbf{q}_n} \end{pmatrix} |0\rangle,$$

$$\bar{f}^\star_n(\mathbf{q}_1, \ldots, \mathbf{q}_n) = g^n N^{(n/2)} \bar{G}^{-1}(\mathbf{k}, \omega) \langle 0| \begin{pmatrix} c_{\mathbf{k}} \\ d_{\mathbf{k}} \end{pmatrix} \hat{G} \begin{pmatrix} e^{-i\xi_{\mathbf{k}-\mathbf{q}_1}} d^\dagger_{\mathbf{k}-\mathbf{q}_T} b^\dagger_{\mathbf{q}_1} B^\dagger_{\mathbf{q}_2} \ldots B^\dagger_{\mathbf{q}_n} & e^{i\xi_{\mathbf{k}-\mathbf{q}_1}} c^\dagger_{\mathbf{k}-\mathbf{q}_T} B^\dagger_{\mathbf{q}_1} b^\dagger_{\mathbf{q}_2} \ldots b^\dagger_{\mathbf{q}_n} \end{pmatrix} |0\rangle.$$

Here, $\mathbf{q}_T = \sum_{i=1}^n \mathbf{q}_i$, and for simplicity of notation we do not write explicitly the $\mathbf{k}$, ω dependence from now on.

We define the total momentum averages $\bar{\mathcal{F}}_n = 1/N^n \sum_{\mathbf{q}_1 \ldots \mathbf{q}_n} \bar{f}_n(\mathbf{q}_1 \ldots \mathbf{q}_n)$, and the partial momentum averages $\delta\bar{f}_n(\mathbf{q}_1) = 1/N^{n-1} \sum_{\mathbf{q}_2 \ldots \mathbf{q}_n} \bar{f}_n(\mathbf{q}_1 \ldots \mathbf{q}_n) - \bar{\mathcal{F}}_n$, $\delta\bar{f}^\star_n(\mathbf{q}_1) = 1/N^{n-1} \sum_{\mathbf{q}_2 \ldots \mathbf{q}_n} \bar{f}^\star_n(\mathbf{q}_1 \ldots \mathbf{q}_n)$. In terms of these, the equations

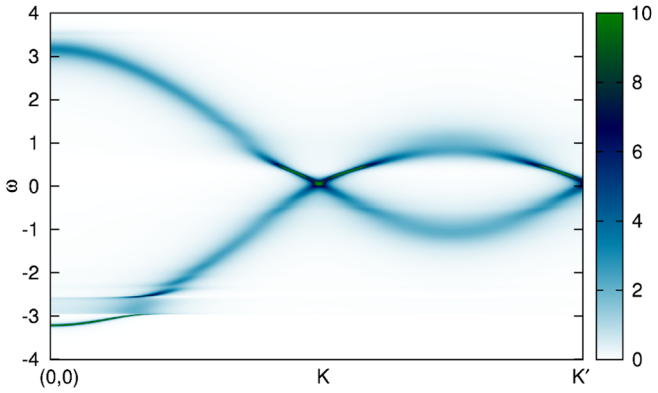

FIG. 1 (color online). Spectral weight along high-symmetry cuts in the Brillouin zone, for $\Omega = 0.25t$ and $\lambda = 0.5$.

of motion are, for any $n \geq 2$

$$\bar{\mathcal{F}}_n = g_{0S,n}(ng^2\bar{\mathcal{F}}_{n-1} + \bar{\mathcal{F}}_{n+1}), \tag{5}$$

$$\delta\bar{f}_n(\mathbf{q}_1) = g_{0S,n}[(n-1)g^2\delta\bar{f}_{n-1}(\mathbf{q}_1) + \delta\bar{f}_{n+1}(\mathbf{q}_1)], \tag{6}$$

$$\delta\bar{f}^{\star}_n(\mathbf{q}_1) = g_{0S,n}[(n-1)g^2\delta\bar{f}^{\star}_{n-1}(\mathbf{q}_1) + \delta\bar{f}^{\star}_{n+1}(\mathbf{q}_1)], \tag{7}$$

where we use the shorthand notation

$$g_{0S,n} \equiv g_{0S}(\omega - n\Omega) = \frac{1}{N}\sum_{\mathbf{k}} G_{0S}(\mathbf{k}, \omega - n\Omega), \tag{8}$$

where the free propagator is given in Eq. (2). For $N \to \infty$, this is a simple 2D integral over the Brillouin zone.

Recurrence equations of the type (5)–(7) have solutions in terms of the continued fractions $A_n(\omega)$ [11]:

$$A_n(\omega) = \frac{ng_{0S,n}}{1 - g^2 g_{0S,n} A_{n+1}(\omega)}. \tag{9}$$

In particular:

$$\bar{\mathcal{F}}_2 = g^2 A_2(\omega)\bar{\mathcal{F}}_1, \tag{10}$$

$$\delta\bar{f}_2(\mathbf{q}_1) = g^2 A_1(\omega - \Omega)\delta\bar{f}_1(\mathbf{q}_1), \tag{11}$$

$$\delta\bar{f}^{\star}_2(\mathbf{q}_1) = g^2 A_1(\omega - \Omega)\delta\bar{f}^{\star}_1(\mathbf{q}_1). \tag{12}$$

These can be combined with the exact equations of motion for the original (rescaled) $\bar{f}_1(\mathbf{q}_1)$ and $\bar{f}^{\star}_1(\mathbf{q}_1)$ one-phonon Green's functions, which read

$$\bar{f}_1(\mathbf{q}_1) = G_{0S}(\mathbf{k} - \mathbf{q}_1, \omega - \Omega)\left[g^2 + \frac{1}{N}\sum_{\mathbf{q}_2}\bar{f}_2(\mathbf{q}_1, \mathbf{q}_2)\right] + G_{0A}(\mathbf{k} - \mathbf{q}_1, \omega - \Omega)\frac{1}{N}\sum_{\mathbf{q}_2}\bar{f}^{\star}_2(\mathbf{q}_1, \mathbf{q}_2), \tag{13}$$

$$\bar{f}^{\star}_1(\mathbf{q}_1) = G_{0A}(\mathbf{k} - \mathbf{q}_1, \omega - \Omega)\left[g^2 + \frac{1}{N}\sum_{\mathbf{q}_2}\bar{f}_2(\mathbf{q}_1, \mathbf{q}_2)\right] + G_{0S}(\mathbf{k} - \mathbf{q}_1, \omega - \Omega)\frac{1}{N}\sum_{\mathbf{q}_2}\bar{f}^{\star}_2(\mathbf{q}_1, \mathbf{q}_2). \tag{14}$$

From these we can easily derive equations for $\bar{\mathcal{F}}_1$, $\delta\bar{f}_1(\mathbf{q}_1)$, $\delta\bar{f}^{\star}_1(\mathbf{q}_1)$ which combined with Eqs. (10)–(12) allow us to calculate all of these quantities. In particular, we find $\bar{\Sigma}_{\mathrm{MA}^{(1)}}(\omega) = \bar{\mathcal{F}}_1 = 1\Sigma_{\mathrm{MA}^{(1)}}(\omega)$; i.e., it is diagonal and momentum independent [13], where

$$\Sigma_{\mathrm{MA}^{(1)}}(\omega) = \frac{g^2 g_{0S}(\tilde{\omega})}{1 - g^2 g_{0S}(\tilde{\omega})[A_2(\omega) - A_1(\omega - \Omega)]} \tag{15}$$

with $\tilde{\omega} = \omega - \Omega - g^2 A_1(\omega - \Omega)$. As a result, we obtain $\bar{G}(\mathbf{k}, \omega) = \bar{G}_0(\mathbf{k}, \omega - \Sigma_{\mathrm{MA}^{(1)}}(\omega))$. This can now easily be extended to lattices with even more complex unit cells.

First, we plot in Fig. 1 the spectral weight $A(\mathbf{k}, \omega) = -\frac{1}{2\pi}\,\mathrm{Im}(\mathrm{Tr}\bar{G}(\mathbf{k}, \omega))$ along high-symmetry cuts in the BZ. This corresponds to fairly weak electron-phonon interactions, with an effective coupling $\lambda = g^2/(3t\Omega) = 0.5$. The effective coupling is defined such that the crossover from large to small polarons is observed for $\lambda \sim 1$, as usual [7]. As expected, the lowest-energy feature is the sharp polaron band, whose dispersion flattens out just below the polaron + one-phonon continuum. Because its quasiparticle (qp) weight decreases away from $\mathbf{k} = 0$, it is hard to see it in this region. We have verified that all expected behavior of the ground-state energy, qp weight, effective mass, average number of phonons in the cloud, etc., are indeed similar to those expected for Holstein polarons.

Above the polaron band, we see the polaron + one-phonon continuum, plus all higher-energy features which remain centered around the corresponding energies of the free electron. Already there is significant broadening at all higher energies, except near the Dirac points, which continue to be very sharp, indicating long lifetimes.

This is further analyzed in Fig. 2, where we present the imaginary part of the self-energy for two different phonon energies, and for different coupling strengths, in the vicinity of the Dirac points. Since at the $\mathrm{MA}^{(1)}$ level the self-

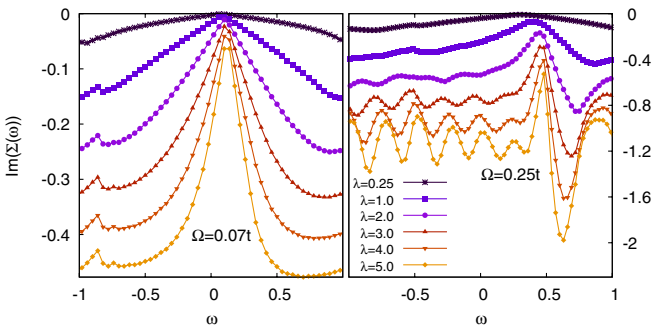

FIG. 2 (color online). Imaginary part of the self-energy for $\Omega = 0.07t$ (left) and $\Omega = 0.25t$ (right).

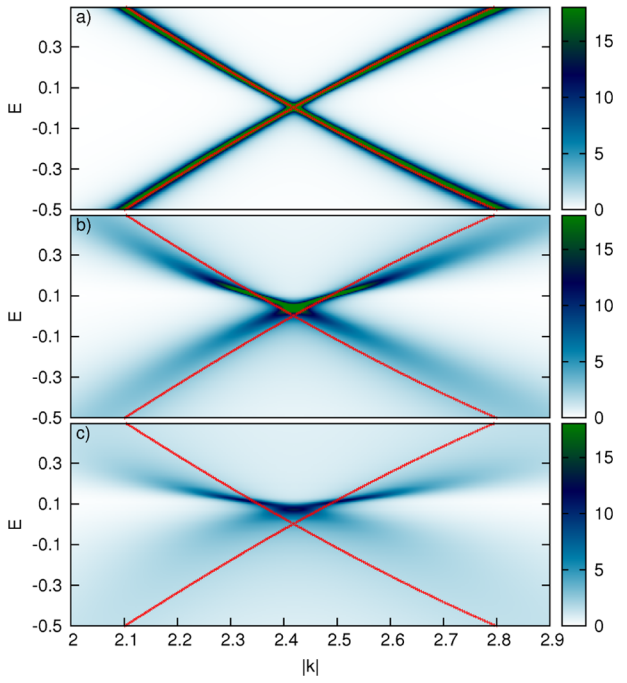

FIG. 3 (color online). Spectral weight near the Dirac points for (a) $\lambda = 0.25$, (b) $\lambda = 2.0$ and (c) $\lambda = 4.0$ and $\Omega = 0.07t$. The red (or gray) lines indicate the free-electron dispersion ($\lambda = 0$).

energy is still momentum independent, the characteristic lifetime is just $\tau \sim -1/\mathrm{Im}(\Sigma)$. The results in Fig. 2 show that as the coupling, and thus the electron-phonon scattering, is increased, lifetimes become shorter and shorter. However, in a relatively narrow energy interval, the lifetimes remain very long even at extremely strong couplings which are well into the small polaron regime. In other words, well-defined Dirac points still exist, although their energy shifts monotonically from $\omega_K = 0$ at weak coupling to $\omega_K \sim 2\Omega$ at strong coupling. Note that for very strong couplings one can also observe the appearance of resonances spaced by Ω, which signal the Lang-Firsov states, expected when $\lambda \to \infty$ [14,15].

Besides the shift in the energy of the Dirac points, we also find significant renormalization (decrease) of the effective "speed of light" with increased coupling. Also, the upper branch has much longer qp lifetimes. These points are illustrated in Fig. 3, where we plot the spectral weight for $\mathbf{k}$ near the K Dirac point at various couplings, together with the free-electron dispersion (red or gray lines). They also agree with the weak-coupling results of Ref. [6].

One may wonder if these results are an artifact due to the $\mathbf{k}$-independent self-energy produced by $\mathrm{MA}^{(1)}$ [13]. This cannot be the case, since $\mathrm{MA}^{(1)}$ obeys exactly 8 spectral weight sum-rules for each value of $\mathbf{k}$, so significant spectral weight shifts necessary for the disappearance of the Dirac points are simply impossible. The explanation for this comes from rewriting Eq. (8) as $g_{0S}(\omega) = \frac{1}{2} \times \int d\epsilon g(\epsilon)[1/(\omega - \epsilon + i\eta) + 1/(\omega + \epsilon + i\eta)]$, where $g(\epsilon)$ is the free-electron density of states (DOS). The largest contributions come from $\epsilon \sim \pm\omega$; however, near the Dirac points $\omega \sim 0$ and the DOS vanishes. As a result, the self-energy of Eq. (15) remains small near (just above) the Dirac points, because $g_{0S}(\tilde{\omega}) \to 0$.

We conclude that well-defined Dirac points are a very robust feature of the graphene, i.e., rather insensitive to rippling effects or, for epitaxial graphene, to the nature of the substrate and the buckling due to mismatching. Experimentally this could be verified by measuring the "speed of light" as a function of type of substrate, or by tuning the coupling to the substrate [16]. This behavior is very fortunate, since it guarantees that the interesting physics expected because of the Dirac points is not affected by such effects. It also explains why rippling can be neglected when studying these quasiparticles, e.g., in their interactions with in-plane phonons [17].

This work was supported by the A. P. Sloan Foundation, CIFAR Nanoelectronics, and NSERC. Discussions with R. Capaz, A. Castro-Neto and G. A. Sawatzky are gratefully acknowledged.

[1] K. S. Novoselov *et al.*, Science **306**, 666 (2004).
[2] A. H. Castro Neto *et al.*, arXiv:cont-mat/0709.1163.
[3] N. D. Mermin, Phys. Rev. **176**, 250 (1968).
[4] J. C. Meyer *et al.*, Nature (London) **446**, 60 (2007).
[5] C. Berger *et al.*, J. Phys. Chem. B **108**, 19 912 (2004).
[6] T. Stauber and N. M. R. Peres, J. Phys. Condens. Matter **20**, 055002 (2008).
[7] For a review, see H. Fehske and S. A. Trugman, in *Polarons in Advanced Materials*, edited by A. S. Alexandrov (Canopus, Bath/Springer-Verlag, Bath, 2007).
[8] A. Macridin *et al.*, Phys. Rev. B **69**, 245111 (2004).
[9] M. Berciu, Phys. Rev. Lett. **97**, 036402 (2006).
[10] G. L. Goodvin, M. Berciu, and G. A. Sawatzky, Phys. Rev. B **74**, 245104 (2006).
[11] M. Berciu and G. L. Goodvin, Phys. Rev. B **76**, 165109 (2007); M. Berciu, Phys. Rev. Lett. **98**, 209702 (2007).
[12] O. S. Barišić, Phys. Rev. Lett. **98**, 209701 (2007).
[13] For Holstein-like coupling, $\mathbf{k}$-dependent self-energy appears from level $\mathrm{MA}^{(2)}$ onwards (see Ref. [11]); however, this has little effect at the high energies of interest here.
[14] I. G. Lang and Y. A. Firsov, Sov. Phys. JETP **16**, 1301 (1963).
[15] Marco Zoli, J. Phys. Condens. Matter **13**, 10 845 (2001).
[16] I. H. Hulea *et al.*, Nat. Mater. **5**, 982 (2006).
[17] Wang-Kong Tse and S. Das Sarma, Phys. Rev. Lett. **99**, 236802 (2007).